Electronic Supplementary Information

Non-stoichiometric Cu-In-S@ZnS Nanoparticles Produced in Aqueous Solutions as Light Harvesters for Liquid-Junction Photoelectrochemical Solar Cells

Alexandra Raevskaya[a], Oksana Rosovik[a], Andriy Kozytskiy[a], Oleksandr Stroyuk[a,*], Volodymyr Dzhagan,[b,c] and Dietrich R. T. Zahn[c]

[a] *L. V. Pysarzhevsky Institute of Physical Chemistry, National Academy of Sciences of Ukraine, Kyiv, 03028, Ukraine*

[b] *V. E. Lashkaryov Institute of Semiconductors Physics, National Academy of Sciences of Ukraine, Kyiv, 03028, Ukraine*

[c] *Semiconductor Physics, Technische Universität Chemnitz, 09107 Chemnitz, Germany*

[*] *Author for correspondence*: Dr. Oleksandr L. Stroyuk, Laboratory of Organic Photovoltaics and Electrochemistry, L.V. Pysarzhevsky Institute of Physical Chemistry, National Academy of Sciences of Ukraine, 31 Nauky av., 03028, Kyiv, Ukraine, tel./fax: +380 44 5250270, e-mail: alstroyuk@ukr.net; stroyuk@inphyschem-nas.kiev.ua

Preparation of the FTO/TiO_2 films. In a typical preparation, 0.45 g ethyl cellulose was dissolved in 9 mL *n*-butanol, then 1.8 g glycerol was added. The solution was refluxed until complete homogenization and mixed with 0.9 g TiO_2 P25 (Evonik Corp.). The suspension was placed in an ultrasound bath for 1 h then refluxed at 80 ^oC for 30 min. The produced paste was deposited onto the FTO as a layer with a thickness equal to one layer of the scotch tape. The films were dried at 70 ^oC for 30 min and annealed at 450 ^oC in air for 1 h.

Details of XPS spectra registration. XPS spectra were acquired under excitation of a 650 μm spot. The monocromized Al K_α ($h\nu$ = 1253.6 eV) X-ray source provided a spectral resolution of 0.5 eV. To prevent possible charging of the sample it was flooded with low kinetic energy electrons (E_{kin} = 0.1 eV, I_{em} = 0.05 mA). Spectra deconvolution and quantification was performed using the Avantage Data System (Thermo Scientific). The number of components used for each spectral decomposition was kept at the minimum required for a meaningful representation of the experimental spectra. A Voigt line shape was used to define the spectral shape of the different components.

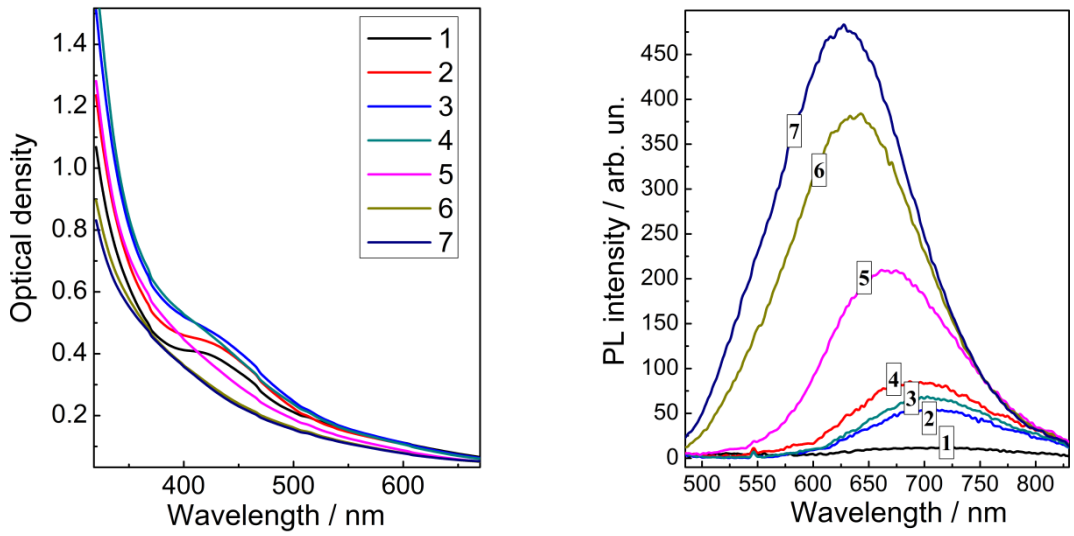

a b

Figure S1. Absorption (a) and PL (b) spectra of CIS (curves 1) and CIS@ZnS NPs produced at a molar Zn:Cu ratio of 0.5 (curve 2), 1 (curves 3), 2 (curves 4), 5 (curves 5), 10 (curves 6), and 20 (curves 7). PL spectra registered at excitation and registration monochromator slits of 15 nm and 2.5 nm, respectively.

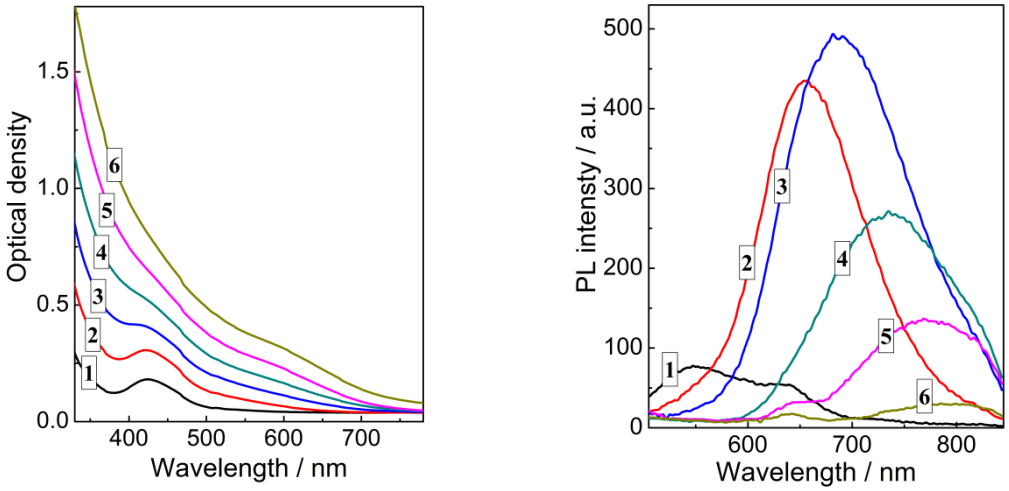

a b

Figure S2. Absorption spectra of CIS NPs (a) and PL spectra of CIS@ZnS NPs produced at fixed In and S contents and a varied molar ratio Cu:In:S = x_{Cu}:5:10 with x_{Cu} = 0.2 (curves 1), 0.6 (2), 1.0 (3), 1.5 (4), 2.0 (5), and 2.5 (6). The Zn:Cu ratio is 1:1. The spectral feature at around 630–640 nm in curves 1,5, and 6 originates from optical cuvette and does not belong to the solutions. PL spectra registered at excitation and registration monochromator slits of 10 nm and 2.5 nm, respectively.

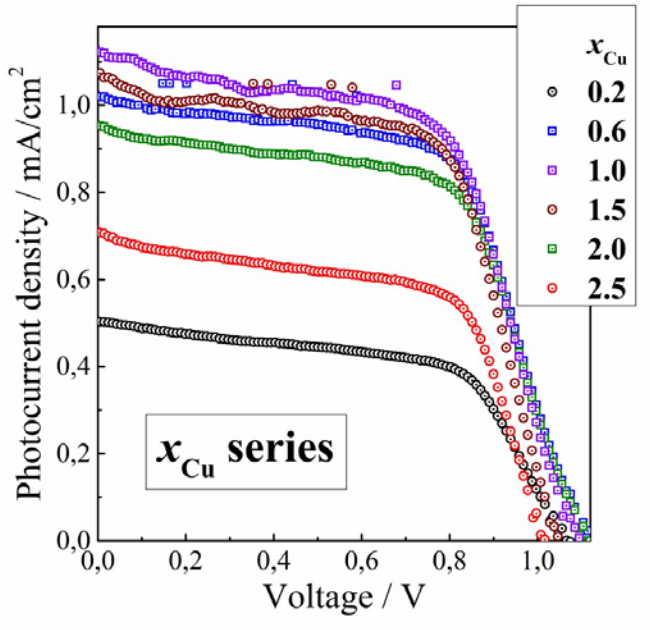

Figure S3. The J–V curves for the three-electrode systems with FTO/TiO_2/CIS photoanodes varying in the copper content x_{Cu}. Other parameters: x_{In} = 5, x_S = 10.

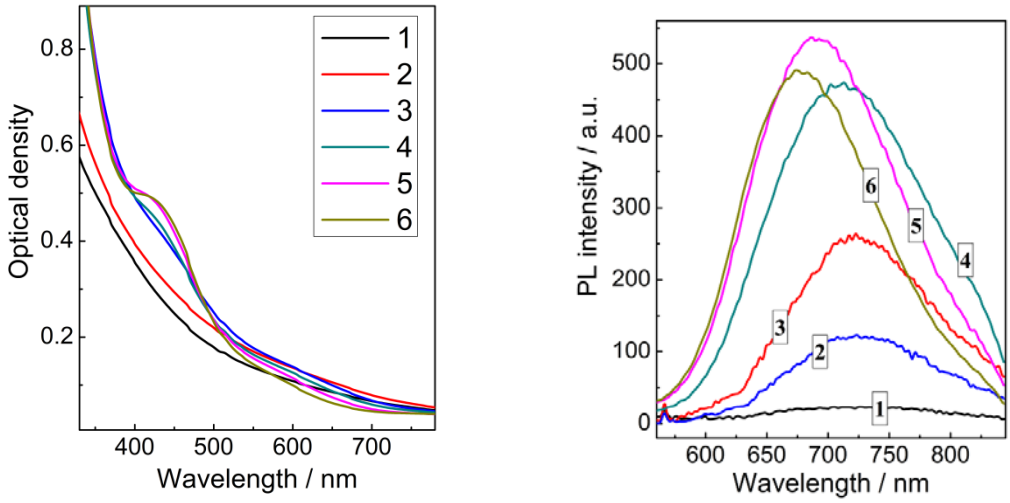

a b

Figure S4. Absorption spectra (a) and PL (b) of CIS@ZnS NPs produced at fixed Cu and S contents and a varied molar ratio Cu:In:S = 1:x_{In}:10 wit x_{In} = 1 (curves 1), 2 (2), 3 (3), 4 (4), 5 (5), and 6 (6). The Zn:Cu ratio is 1:1. PL spectra registered at excitation and registration monochromator slits of 10 nm and 2.5 nm, respectively.

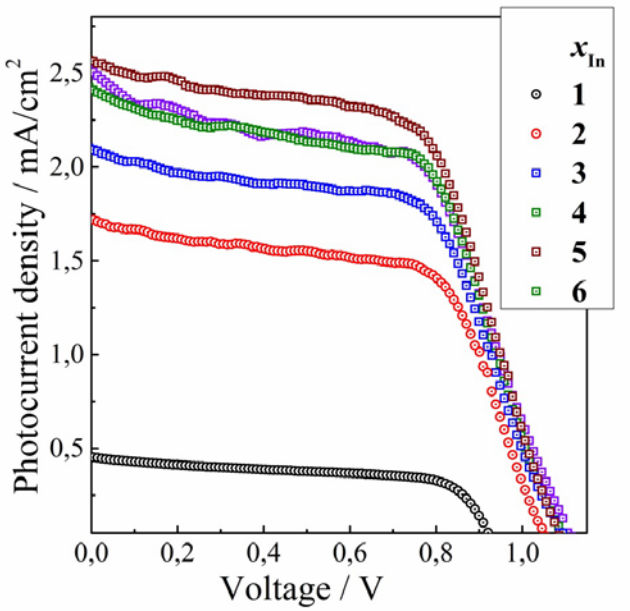

Figure S5. The J–V curves for the three-electrode systems with FTO/TiO_2/CIS photoanodes varying in the indium content x_{In}. Other parameters: x_{Cu} = 1, x_S = 10.

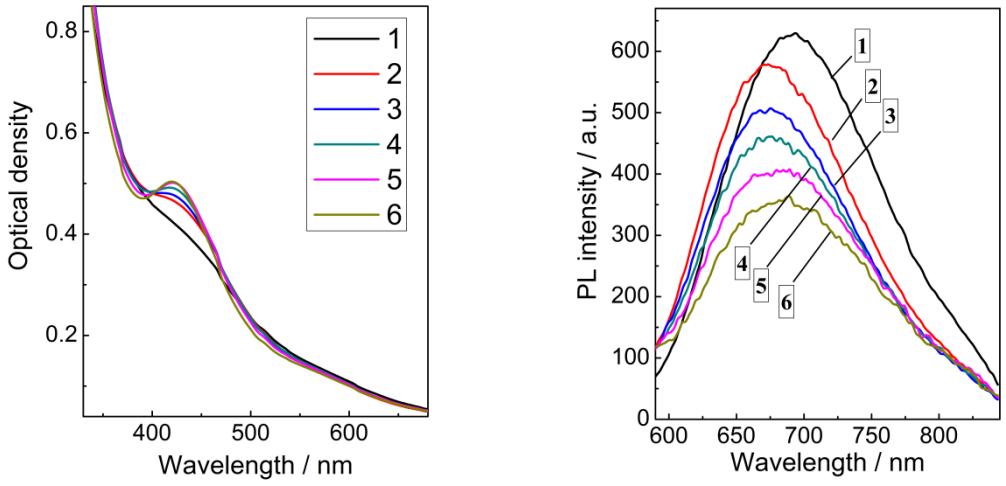

a b

Figure S6. Absorption spectra (a) and PL (b) of Cu-In-S@ZnS NPs produced at fixed Cu and In contents and a varied molar ratio Cu:In:S = 1:5:x_S with x_S = 7 (curves 1), 9 (curves 2), 10 (curves 3), 11 (curves 4), 13 (curves 5), and 15 (curves 6). The Zn:Cu ratio is 1:1.

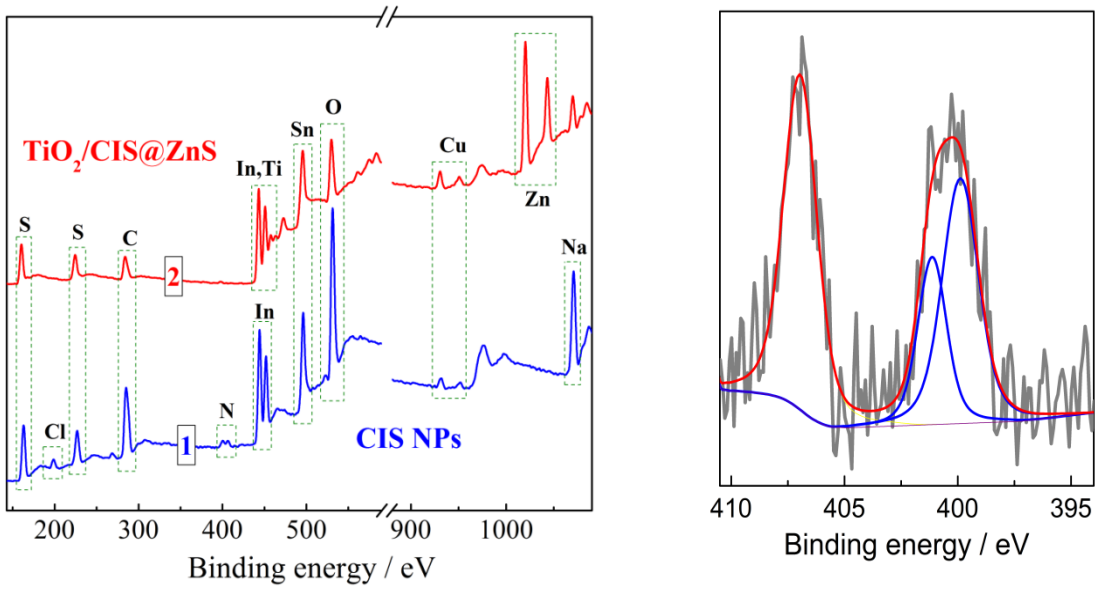

a b

Figure S7. (a) XPS survey spectra of CIS NPs (curve 1) and TiO_2/CIS@ZnS heterostructure (2); (b) high-resolution XPS spetrum of the N1s range of CIS NPs.

Table S1. Atomic fractions of Cu and In in CIS NPs, CIS@ZnS NPs and TiO_2/CIS@ZnS heterostructure determined from the XPS survey spectra

Sample	Cu, at.%	In, at. %	Cu:In
CIS NPs	3.0	15.7	1:5.2
CIS@ZnS NPs	2.5	12.3	1:4.9
TiO_2/CIS@ZnS	1.8	8.7	1:4.8

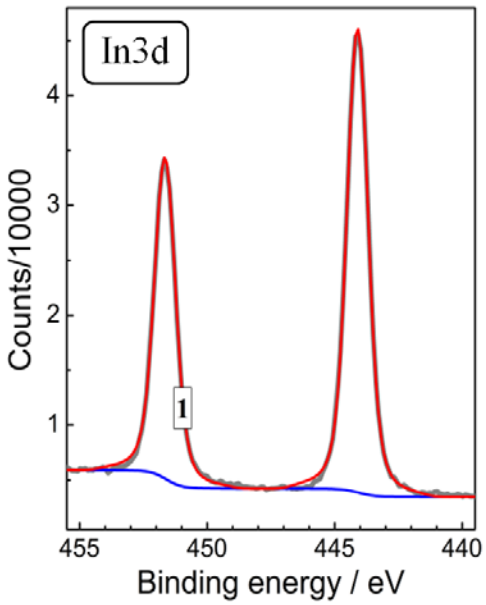

Figure S8. High resolution X-ray photoelectron spectra of CIS NPs in the range of In3d signal. Cu:In:S = 1:5:10, Zn:Cu = 10:1.

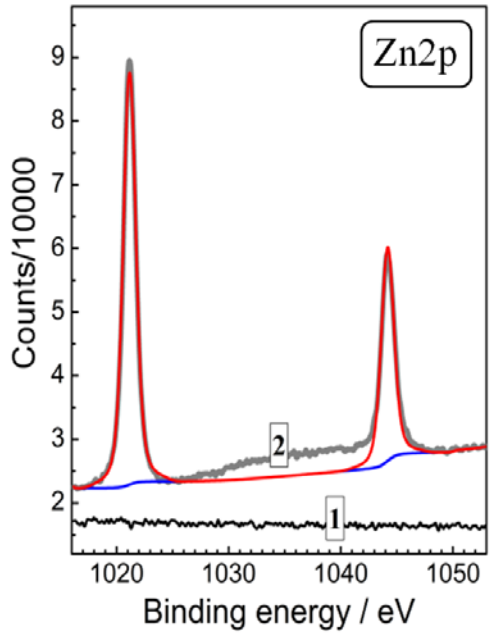

Figure S9. High resolution X-ray photoelectron spectra of CIS@ZnS NPs in the range of Zn2p signal. Cu:In:S = 1:5:10, Zn:Cu = 10:1.

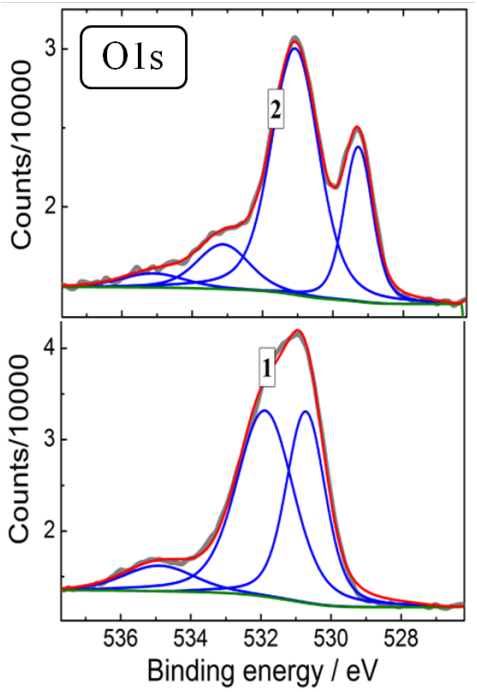

Figure S10. High resolution XPS spectra of CIS NPs drop casted on Si (curve 1) and CIS@ZnS NPs as a part of TiO_2/CIS@ZnS photoanode (curves 2) in the range of O1s signal.

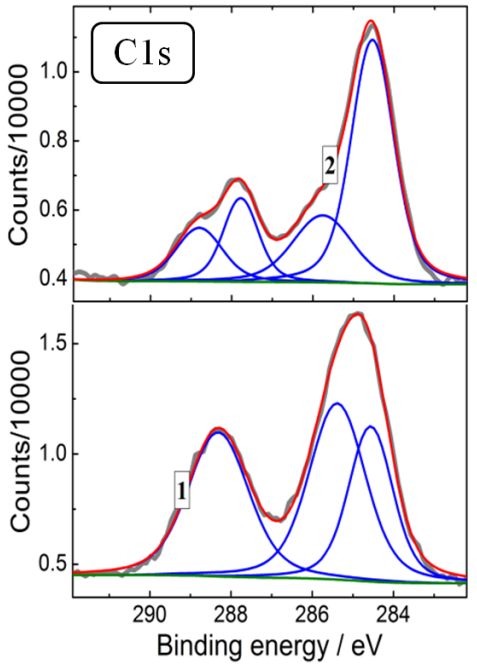

Figure S11. High resolution XPS spectra of CIS NPs drop casted on Si (curve 1) and CIS@ZnS NPs as a part of TiO_2/CIS@ZnS photoanode (curves 2) in the range of C1s signal.

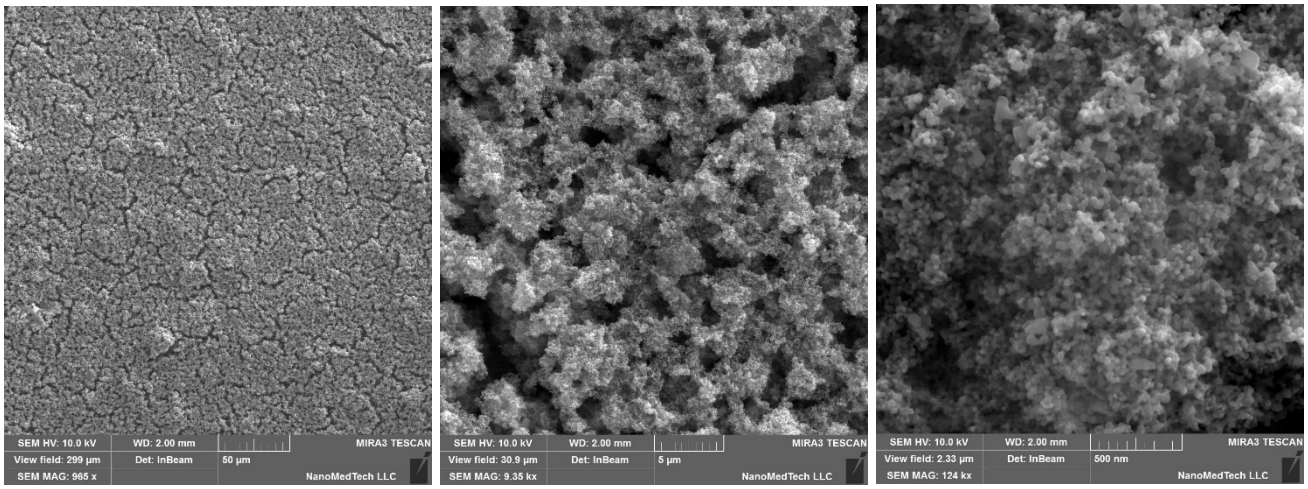

Figure S12. SEM images of FTO/TiO_2 film registered at different magnification.

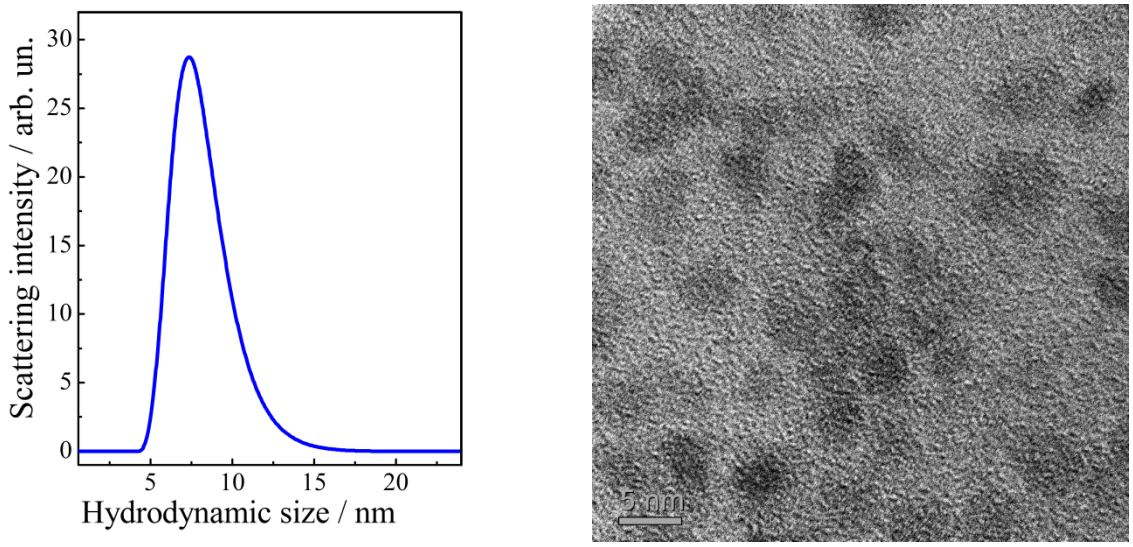

a b

Figure S13. (a) Distribution of CIS@ZnS NPs by the hydrodynamic size in original colloidal solutions used for the preparation of optimized TiO_2/CIS@ZnS photoanode. The dynamic light scattering measurements were performed with a Zetasizer Nano (Malvern Instruments). The solvent viscosity was measured with a Malvern SV-100 vibrational viscometer. The refractive index of bulk $CuInS_2$ was used in all DLS measurements. (b) TEM image of CIS@ZnS NPs. The image was registered on a Philips CM 20 FEG microscope at an accelerating voltage of 200 kV.

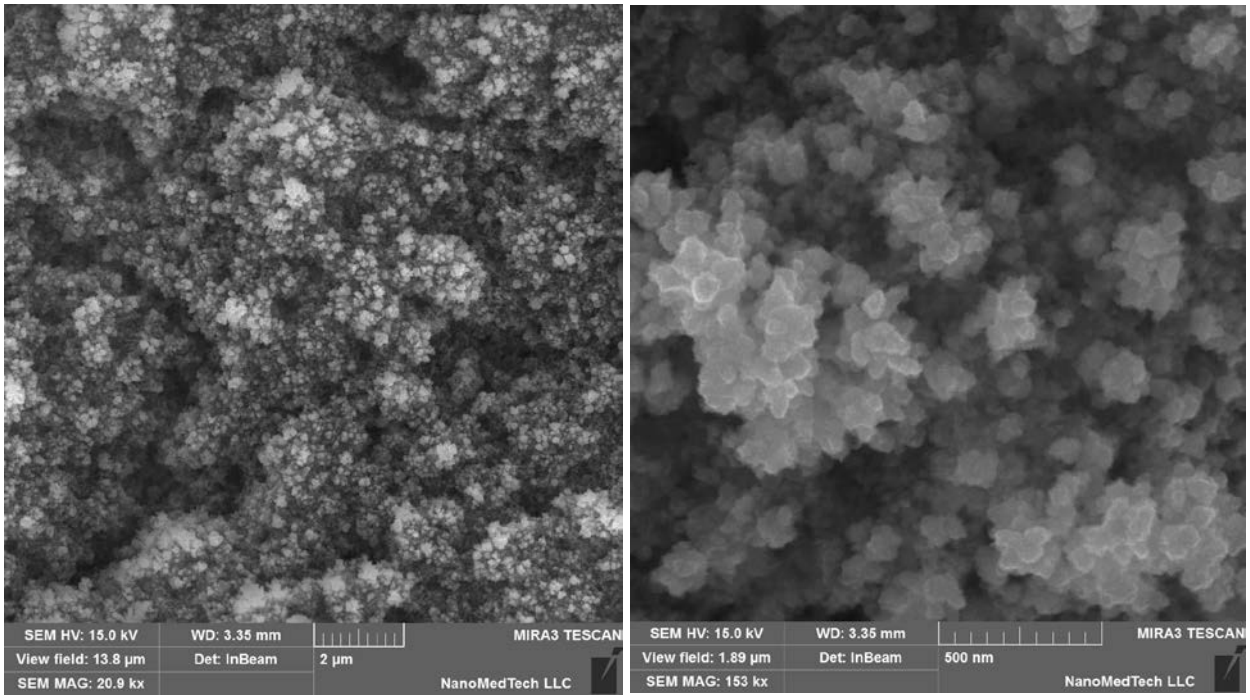

Figure S14. SEM images of FTO/TiO_2/Cu^0 film produced by photocatalytic reduction of Cu^{II} with ethanol.

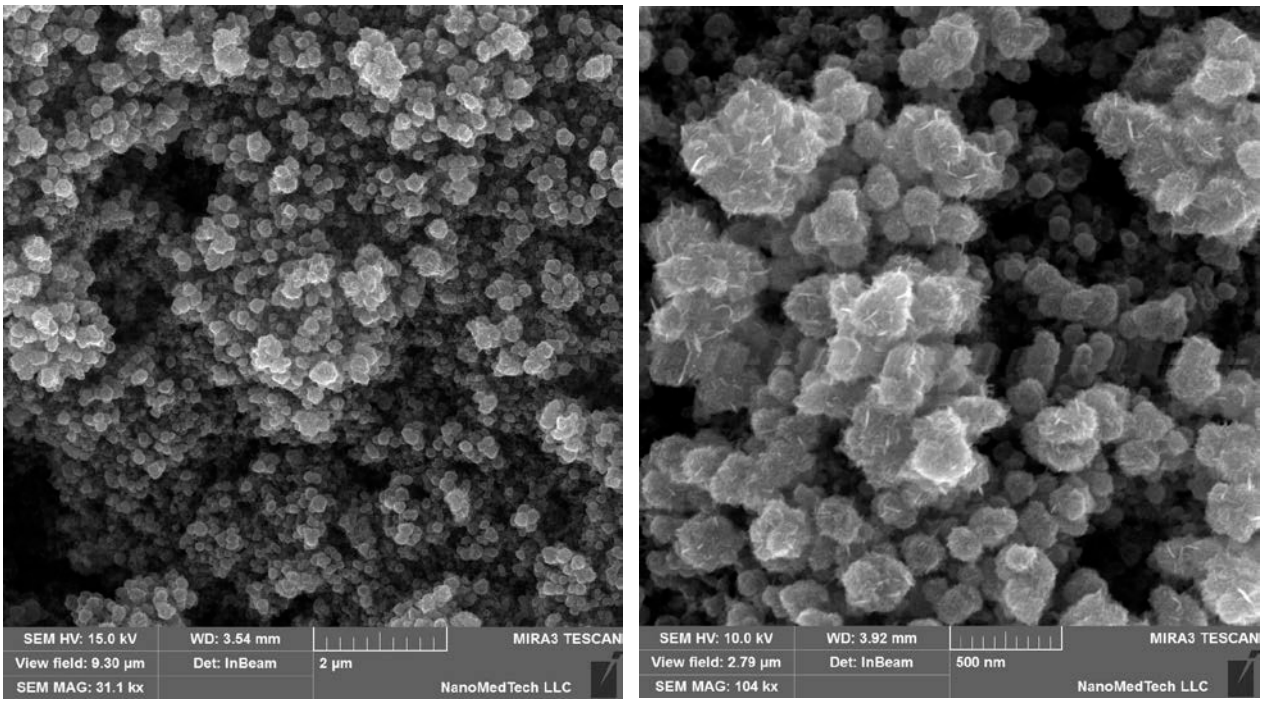

Figure S15. SEM images of TiO_2/Cu_2S film produced by sulfurization of TiO_2/Cu^0 heterostructure

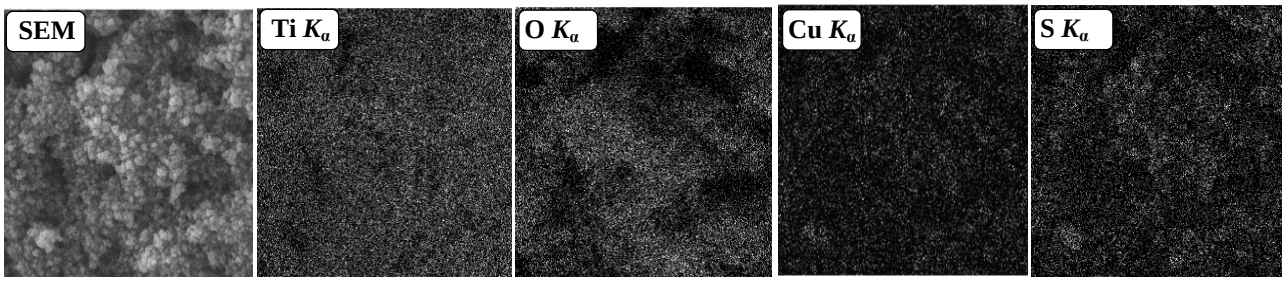

a b c d e

Figure S16. SEM image of TiO_2/Cu_2S film (a) and corresponding distribution maps of titanium (b), oxygen (c), copper (d), and sulfur (e) as revealed by EDX analysis.